SCIENCE CHINA
Chemistry

•COMMUNICATIONS•

May 2021 Vol.64 No.5: 739–744
https://doi.org/10.1007/s11426-020-9980-4

Ultralong organic room-temperature phosphorescence of electron-donating and commercially available host and guest molecules through efficient Förster resonance energy transfer

Yeling Ning[1], Junfang Yang[2], Han Si[1], Haozhong Wu[1], Xiaoyan Zheng[2*], Anjun Qin[1*] & Ben Zhong Tang[1,3]

[1]*State Key Laboratory of Luminescent Materials and Devices, Guangdong Provincial Key Laboratory of Luminescence from Molecular Aggregates, SCUT-HKUST Joint Research Institute, AIE Institute, Center for Aggregation-Induced Emission, South China University of Technology (SCUT), Guangzhou 510640, China;*

[2]*Beijing Key Laboratory of Photoelectronic/Electrophotonic Conversion Materials, Key Laboratory of Cluster Science of Ministry of Education, Beijing Institute of Technology, Beijing 100081, China;*

[3]*Department of Chemistry, Hong Kong Branch of Chinese National Engineering Research Center for Tissue Restoration and Reconstruction, Institute for Advanced Study, and Department of Chemical and Biological Engineering, The Hong Kong University of Science & Technology (HKUST), Clear Water Bay, Kowloon, Hong Kong, China*

Received December 3, 2020; accepted March 15, 2021; published online March 23, 2021

Ultralong organic room-temperature phosphorescence (RTP) materials have attracted tremendous attention recently due to their diverse applications. Several ultralong organic RTP materials mimicking the host-guest architecture of inorganic systems have been exploited successfully. However, complicated synthesis and high expenditure are still inevitable in these studies. Herein, we develop a series of novel host-guest organic phosphorescence systems, in which all luminophores are electron-rich, commercially available and halogen-atom-free. The maximum phosphorescence efficiency and the longest lifetime could reach 23.6% and 362 ms, respectively. Experimental results and theoretical calculation indicate that the host molecules not only play a vital role in providing a rigid environment to suppress non-radiative decay of the guest, but also show a synergistic effect to the guest through Förster resonance energy transfer (FRET). The commercial availability, facile preparation and unique properties also make these new host-guest materials an excellent candidate for the anti-counterfeiting application. This work will inspire researchers to develop new RTP systems with different wavelengths from commercially available luminophores.

room-temperature phosphorescence, host-guest system, Förster resonance energy transfer, commercial luminophore, anti-counterfeiting

Citation: Ning Y, Yang J, Si H, Wu H, Zheng X, Qin A, Tang BZ. Ultralong organic room-temperature phosphorescence of electron-donating and commercially available host and guest molecules through efficient Förster resonance energy transfer. *Sci China Chem*, 2021, 64: 739–744, https://doi.org/10.1007/s11426-020-9980-4

Room-temperature phosphorescence (RTP) materials have drawn tremendous attention because of their distinctive photophysical properties such as long emission lifetime and the excited state energy, which can be widely applied in data encryption, anti-counterfeiting, background-free bioimaging, chemical sensors, and so on [1–7]. Although inorganic phosphorescence materials such as luminous pearls and glow-in-the-dark stones are abundant on the earth, most of them suffer from some intrinsic problems, including high cost, potential toxicity, and low biocompatibility. For example, a highly efficient RTP system of $SrAl_2O_4$ doped with europium and dysprosium was developed in the mid-1990s,

*Corresponding authors (email: xiaoyanzheng@bit.edu.cn; msqinaj@scut.edu.cn)

and this inorganic system formed the basis of most commercial glow-in-the-dark paints because of its long emission time (>10 h) and high durability [8]. However, this system requires not only rare-earth elements for the long-lived emission but also very high fabrication temperature (>1,000 °C). Moreover, the manufacture of the paints from the insoluble $SrAl_2O_4$ requires tedious procedures, including grinding of the compounds into micrometer-scale powders for dispersing into solvents or matrices. Moreover, the light scattering effect by the powders prevents the formation of transparent paints [9]. It is thus urgent to explore other counterparts with extraordinary features.

With the endeavors paid by the scientists, purely organic phosphorescence materials by the introduction of heavy halogen atoms, carbonyls groups or some heteroatoms, hydrogen bonding, H-aggregation, strong intermolecular electronic coupling, molecular packing *etc*., have been reported [3,6,10–20]. Moreover, ultralong organic phosphorescence materials through imitating the host-guest architecture of minerals were also developed [21–23], which are inspired by the generally accepted principle in inorganic RTP systems where impurities are responsible and involved in the three steps: (1) excitation of the guest species (impurity), (2) trapping of the excited electrons by defects in host matrices, and (3) slow charge recombination of the trapped electrons by thermal energy [24]. However, complicated synthesis and high expenditure are still inevitable in these systems. In addition, their performances in air are not satisfactory and the introduction of halogen atoms is generally necessary. For example, Adachi *et al*. [25] obtained a purely organic afterglow lasting for more than 1 h *via* blending one electron-donating guest in an electron-withdrawing host, but the overall emission quantum yield was only 7% in air. Tang *et al*. [26] developed a series of purely organic host-guest materials which are electron-deficient, and have halogen atoms, carbonyl groups and cyano units. Therefore, a new facile and robust host-guest strategy utilizing only electron-rich materials is a promising alternative for constructing RTP systems.

We accidentally observed a notable RTP phenomenon in a routing experiment by mixing *N*,*N*,*N*′,*N*′-tetraphenylbenzidine (TPB), triphenylamine (TPA) and triphenylphosphine (TPP) (Figure 1(a)). As we all know, TPA and TPP are commonly used starting reagents in organic experiments, and TPB is a widely employed hole-transporting material in organic light-emitting diodes (OLEDs) [27]. In other words, all these three molecules are commercially available with low cost. Moreover, they are electron-rich and do not contain halogen atoms. When TPB was doped into TPA or TPP and formed co-crystals, in which TPB acted as a guest, while TPA and TPP served as hosts, the maximum phosphorescence quantum yield (Φ_P) and the longest lifetime could reach 23.6% and 362 ms, respectively. Furthermore, the experimental results and theoretical calculation revealed that the host molecules not only play a vital role in providing a rigid environment and suppressing non-radiative decay of the guest, but also show a synergistic effect to the guest in the photophysical process, where Förster resonance energy transfer (FRET) is a key issue to facilitate the phosphorescence of TPB [28–32]. These new host-guest RTP systems enjoying the integrated merits such as commercially available compounds with electron-rich features and low cost, absence of halogen atoms, facile preparation and excellent performances, will attract wide attentions and inspire further innovation.

To avoid any possible interference of impurities of the TPB, TPA and TPP, strict purification procedures including column chromatography and recrystallization for three times were used, and their purity is unambiguously confirmed by high performance liquid chromatography (HPLC) measurement (Figure S1). Afterward, the photophysical properties of the individual component and guest-host systems are investigated at room temperature (Figure 1(b)).

TPB in the crystalline state exhibits a violet blue fluorescence with the peak at 422 nm and a lifetime of 1.3 ns (Table 1 and Figure S2). Meanwhile, a very weak phosphorescence at 530 nm and a lifetime of 9.7 μs under ambient condition are recorded. The biphenyl core with a torsion angle of 32.9° is verified to be the origin of RTP after the comparison of various fragments of the molecular family of TPB (Figure S3 (a)) [33,34]. Moreover, the C–H···π intermolecular interactions with the distance of 2.780–3.767 Å which effectively restrict the molecular rotation and decrease the nonradiative decay, also contribute to the RTP (Figure S3(b)).

Unique luminescence properties were also observed on TPP crystalline powders. As shown in Figure 1(b) and Figure S4, an obvious fluorescence emission peak at 285 nm was recorded in the photoluminescence (PL) spectra of TPP in tetrahydrofuran (THF) solution, while no emission peak was found in its solid state. Meanwhile, the emission peak at 439 nm in its crystalline state was recorded and readily assignable to be phosphorescence owing to the long lifetime of 1.4 μs (Figure S5). Furthermore, this emission peak was further proven by measuring its PL spectrum at 77 K (Figure S6), from which a similar emission profile was obtained. It is worth noting that, different from TPP, TPA only emits fluorescence with a peak at 393 nm, and no phosphorescence was recorded at room temperature.

The PL quantum yield (Φ_{PL}) measurements indicated that the crystals of TPP and TPA showed weak luminescence with overall values of 4.6% and 9.7%, respectively. However, when 1.0 mol% TPB was doped, the formed TPB/TPP and TPB/TPA co-crystals, which were confirmed *via* X-ray diffraction (Figure S7), exhibited enhanced Φ_{PL} (Table 1). Notably, the formation of co-crystalline structures was further confirmed by differential scanning calorimetry (DSC)

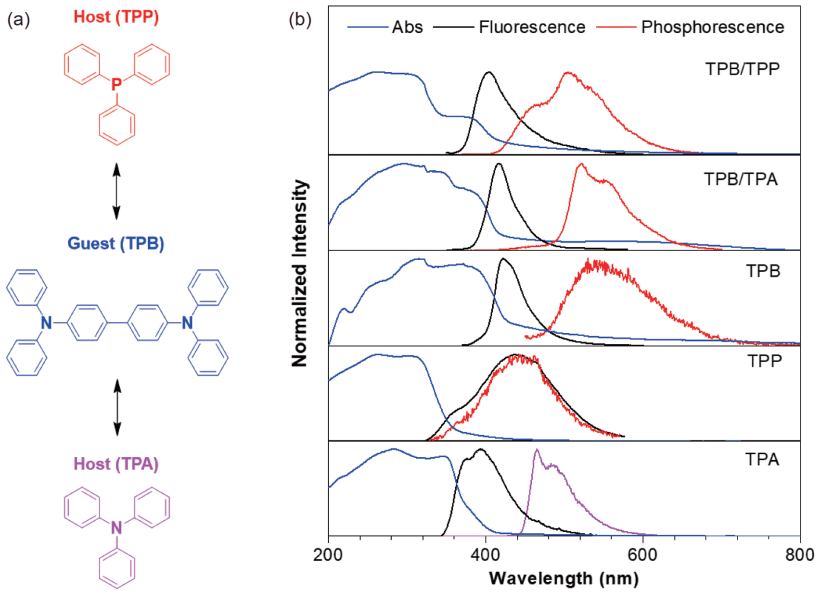

Figure 1 (a) The chemical structures of host and guest molecules. (b) Absorption, photoluminescence and phosphorescence spectra of TPA, TPP, TPB, 1.0 mol% TPB/TPA and 1.0 mol% TPB/TPP crystalline powders at room temperature. The phosphorescence spectra of TPA was obtained at 77 K in purple line (color online).

Table 1 Photophysical properties of host, guest molecules and their doped compounds [a)]

Sample	Φ_{PL} [b)] (%)	$\lambda_{em,Fluo}$ (nm)	τ (ns)	$\lambda_{em,Phos}$ (nm)	Φ_P (%)	τ (ms)
TPB	22.9	422	1.3	530	/	0.0097
TPP	4.6	285 [c)]	0.6 [d)]	439	/	0.0014
TPA	9.7	393	2.7	465 [e)]	/	/
TPB/TPP	45.8	404	1.4	505/540	23.6	336/362 [f)]
TPB/TPA	41.6	417	1.7	522/552	19.4	198/199 [g)]

a) Guest/host=1:100 (molar ratio). b) PL quantum yield of samples. c) Fluorescence emission of TPP in tetrahydrofuran (THF). d) Fluorescence lifetime of TPP in THF. e) Data were collected at 77 K. f) Data were measured at the wavelengths of 505 and 540 nm, respectively. g) Data were measured at the wavelengths of 522 and 552 nm, respectively.

measurement, from which only one melting point of TPB/TPP and TPB/TPA, different from that of TPP and TPA themselves, was recorded (Figure S8). Moreover, the quantum yields of the ground powders of TPB/TPP and TPB/TPA decreased compared with the original ones (Table S1 and Figure S9), further confirming the crystalline nature of the host-guest systems.

The PL measurements (Figure 1(b)) showed that TPB/TPP and TPB/TPA co-crystals gave purple fluorescence with the peaks at 404 and 417 nm, respectively. Meanwhile, the maximum phosphorescence peak of TPB/TPP and TPB/TPA was recorded at 505 and 522 nm, with a shoulder peak at 458 and 540 nm, and 552 nm, respectively, which were almost consistent with the phosphorescence profiles measured at 77 K (Figure S10). It is worth noting that no obvious change for PL upon excitation with different wavelengths was observed for the co-crystals, suggesting that the emission originates from the same species (Figure S11).

Delayed time-resolved photoluminescence spectra displayed that the longest RTP lifetime of TPB/TPP and TPB/TPA could reach 362 and 199 ms for their shoulder peaks at 540 and 552 nm, respectively (Figure S12). Meanwhile, the lifetime for their maximum peaks at 505 and 522 nm was slightly shortened, which may be ascribed to the difference of excited states [14]. As a result, a greenish afterglow that lasts for several seconds was observed from both of the co-crystals under ambient conditions. Excitingly, the co-crystals of TPB/TPP and TPB/TPA gave high Φ_P values of 23.6% and 19.4%, respectively. The relatively stronger Φ_p value of TPB/TPP than that of TPB/TPA might be due to the atomic effect of phosphorus in the former case.

In general, the host materials only provide a rigid environment to prevent the triplet excitons from quenching by the interaction with oxygen. However, the lifetime of co-crystals of TPB/TPP and TPB/TPA at room temperature just enhanced slightly under nitrogen compared with that in air (Figure S13). Therefore, the great luminous ability of the host-guest systems under ambient conditions indicates that the rigid host molecules also restrict the motion of the guest ones and decrease the non-radiation transitions, thus improving the light-emitting efficiency.

To have a deep insight into aforementioned phenomena and to obtain the singlet and triplet energy levels of the host and guest molecules, density functional theory calculations were performed. As shown in Figure 2(a), the electronic density of the major transition orbitals (the highest occupied molecular orbital and the lowest unoccupied molecular or-

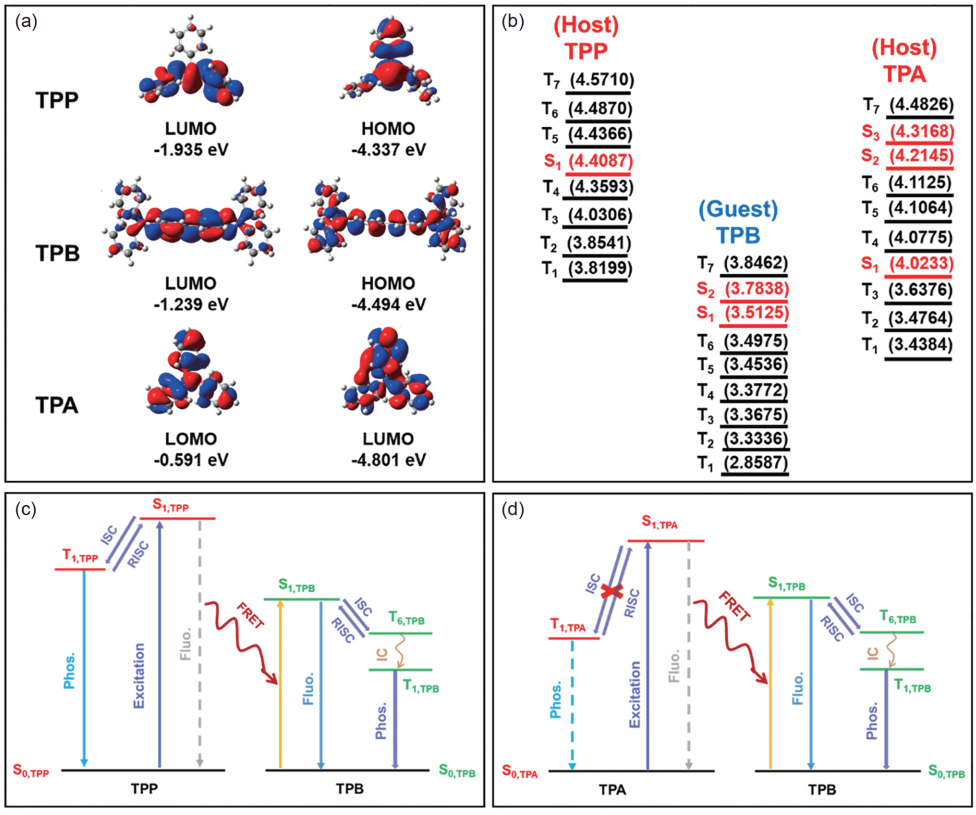

Figure 2 (a) Molecular orbitals and the corresponding energies of TPP, TPB and TPA calculated by B3LYP/6-31G(d,p). (b) Theoretical energy level diagrams of TPP, TPB and TPA based on crystal data. Schematic diagram of PL processes for (c) TPB/TPP and (d) TPB/TPA guest-host systems (color online).

bital (HOMO and LUMO)) of TPB are mainly located on the biphenyl cores, which is consistent with the reported experimental results [33], substantiating the reliability of the calculation. Moreover, the calculated results manifested that the spin−orbit coupling constant (SOC, $\xi(S_1,T_1)$) of the TPB was only 0.05 cm^{-1} due to the lack of heavy atoms [10,11,35], which is consistent with the short lifetime and low quantum yield of its single component. However, the persistent RTP can be generated by doping the TPB into either TPP or TPA host. It means that the host and guest molecules must act synergistically in the photo-excited electronic transitions. Thus, the energy levels of TPB, TPP and TPA were calculated. As displayed in Figure 2(b), a large energy gap between the lowest singlet state (S_1) and lowest triplet state (T_1) of guest molecules does not facilitate the intersystem crossing (ISC). Given the big proportion of the spectral overlap between the emission of the host and the absorption of the guest (Figure S14) and previous reports [28–32], we can conclude that the FRET process exists in these host-guest systems, in which TPP or TPA acts as an energy donor and TPB as an acceptor [36], respectively. Additionally, the FRET process between TPB and TPP or TPA could be largely promoted for their short distance in co-crystals in order to facilitate efficient intermolecular interactions [31,32].

The efficiency of the FRET is usually measured by the energy transfer rate from a host (donor) to a guest (acceptor) (k_{ET}), the efficiency (Φ_{ET}) and the Förster radius (R_0), at which the FRET is 50% efficient. The k_{ET} can be calculated using the following equation [37]:

$$k_{ET} = \frac{1}{\tau_D}\left(\frac{R_0}{R_{DA}}\right)^6 \quad (1)$$

where τ_D is the decay lifetime of a host in the absence of a guest, R_0 is the Förster distance, and R_{DA} is the host-to-guest distance [38]. The efficiency of energy transfer Φ_{ET} is given by the following expression:

$$\Phi_{ET} = \frac{k_{ET}}{k_{ET}+\frac{1}{\tau_D}} = \frac{1}{1+\left(\frac{R_{DA}}{R_0}\right)^6} \quad (2)$$

The calculated R_0, k_{ET} and Φ_{ET} of our host–guest systems are listed in Table 2. It is evident that the Φ_{ET} of the TPB/TPA system (91.50%) is much higher than that of the TPB/TPP (74.33%) one. The great distinction of Φ_{ET} reveals that TPB/TPA co-crystals experienced an absolute FRET process so that no emission originating from TPA appeared in the phosphorescence spectrum. By contrast, TPB/TPP co-crystals underwent an incomplete FRET process following an efficient intersystem crossing from the singlet state of TPP to

triplet states, thus causing the extra shoulder peak at 458 nm originating from the phosphorescence of TPP. Consequently, persistent RTP systems through a host-guest strategy involving efficient FRET could well occur in different systems as plotted in Figure 2(c, d).

After having a deep understanding of the mechanism, we demonstrated the potential application of these host-guest systems. Since the guest can be mixed into the hosts at the molecular level through a facile evaporation process to show ultrolong RTP, these co-crystals are of great potential to serve as anti-counterfeiting materials [39]. Considering the similar purple fluorescence color of TPB, TPB/TPP and TPB/TPA crystals, and the doped materials all exhibited bright green phosphorescence with various lifetimes of afterglow (Figure 3(a)), an anti-counterfeiting pattern "888" was fabricated using different luminophores (Figure 3(b)). Under a 365 nm UV-lamp irradiation, the pattern displayed a digital number "888", which became an obvious word "UOP" (which means Ultralong Organic Phosphorescence) visible to the naked eyes due to the synergistic emission of TPB/TPP and TPB/TPA co-crystals after ceasing UV light irradiation instantly. At the end, the digital number of "111" emitting from TPB/TPP appeared after 2 s (Figure 3(c)). Hence, triple data encryption processes were realized by this simple preparation method, which would be much promising in practical applications.

In summary, a purely organic RTP with high-efficiency and ultralong lifetime was realized *via* mixing a commercially available TPB guest into an TPP or TPA host. The experimental results and theoretical simulation indicate that: (1) the host molecules not only play a vital role in avoiding the quenching of the triplet excited states by oxygen, but also restrain the non-radiation transitions to advance the light-emitting efficiency; (2) host and guest molecules work synergistically in the photo-excited electronic transition processes; (3) an efficient FRET process is activated in the co-crystals of the host and guest to facilitate the luminescence originating from TPB. This strategy enjoys the advantages including low cost, absence of halogen atoms, facile preparation and excellent performances, which shows great potentials in practical applications. Therefore, this work broadens the way for the fabrication of purely organic RTP materials and offers a novel platform for the development of diverse applications. It is envisioned that if the host and guest molecules with longer emissive wavelengths and suitable energy levels are used, persistent RTP with longer emission wavelengths might be realized through this strategy.

Table 2 Förster resonance energy transfer parameters of the host–guest systems [a)]

Host	Guest	R_0 (nm)	k_{ET} (s^{-1})	Φ_{ET} (%)
TPP	TPB	2.60	4.83×10^9	74.33
TPA	TPB	3.17	3.98×10^9	91.50

a) The detailed computational processes are shown in the Supporting Information.

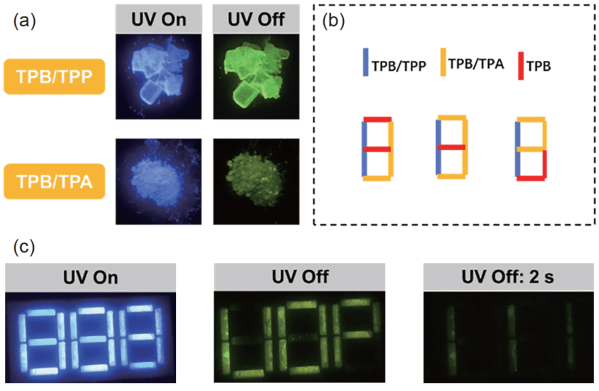

Figure 3 (a) 1.0 mol% TPB/TPP and TPB/TPA crystalline powders before and after the removal of 365 nm UV irradiation. (b) Patterns designed with different phosphors. (c) Demonstration of triple anti-counterfeiting using the TPB/TPP, TPB/TPA and TPB crystals (color online).

Acknowledgements This work was supported by the National Natural Science Foundation of China (21788102 and 21525417), the Natural Science Foundation of Guangdong Province (2019B030301003 and 2016A030312002), and the Innovation and Technology Commission of Hong Kong (ITC-CNERC14S01).

Conflict of interest The authors declare no conflict of interest.

Supporting information The supporting information is available online at http://chem.scichina.com and http://link.springer.com/journal/11426. The supporting materials are published as submitted, without typesetting or editing. The responsibility for scientific accuracy and content remains entirely with the authors.

1 Liu W, Wang J, Gong Y, Liao Q, Dang Q, Li Z, Bo Z. *Angew Chem Int Ed*, 2020, 59: 20161–20166
2 He Z, Gao H, Zhang S, Zheng S, Wang Y, Zhao Z, Ding D, Yang B, Zhang Y, Yuan WZ. *Adv Mater*, 2019, 31: 1807222
3 Su Y, Phua SZF, Li Y, Zhou X, Jana D, Liu G, Lim WQ, Ong WK, Yang C, Zhao Y. *Sci Adv*, 2018, 4: eaas9732
4 Zhang KY, Yu Q, Wei H, Liu S, Zhao Q, Huang W. *Chem Rev*, 2018, 118: 1770–1839
5 Yang J, Gao H, Wang Y, Yu Y, Gong Y, Fang M, Ding D, Hu W, Tang BZ, Li Z. *Mater Chem Front*, 2019, 3: 1391–1397
6 Yang Z, Xu C, Li W, Mao Z, Ge X, Huang Q, Deng H, Zhao J, Gu FL, Zhang Y, Chi Z. *Angew Chem Int Ed*, 2020, 59: 17451–17455
7 Bian L, Ma H, Ye W, Lv A, Wang H, Jia W, Gu L, Shi H, An Z, Huang W. *Sci China Chem*, 2020, 63: 1443–1448
8 Matsuzawa T, Aoki Y, Takeuchi N, Murayama Y. *J Electrochem Soc*, 1996, 143: 2670–2673
9 Li Y, Gecevicius M, Qiu J. *Chem Soc Rev*, 2016, 45: 2090–2136
10 Shi H, Song L, Ma H, Sun C, Huang K, Lv A, Ye W, Wang H, Cai S, Yao W, Zhang Y, Zheng R, An Z, Huang W. *J Phys Chem Lett*, 2019, 10: 595–600
11 Wang J, Gu X, Ma H, Peng Q, Huang X, Zheng X, Sung SHP, Shan G, Lam JWY, Shuai Z, Tang BZ. *Nat Commun*, 2018, 9: 2963
12 Cai S, Shi H, Tian D, Ma H, Cheng Z, Wu Q, Gu M, Huang L, An Z, Peng Q, Huang W. *Adv Funct Mater*, 2018, 28: 1705045
13 Lucenti E, Forni A, Botta C, Carlucci L, Giannini C, Marinotto D, Pavanello A, Previtali A, Righetto S, Cariati E. *Angew Chem Int Ed*, 2017, 56: 16302–16307
14 He Z, Zhao W, Lam JWY, Peng Q, Ma H, Liang G, Shuai Z, Tang BZ.

Nat Commun, 2017, 8: 416–423
15 Song X, Zhang D, Huang T, Cai M, Duan L. *Sci China Chem*, 2018, 61: 836–843
16 Yang Z, Mao Z, Zhang X, Ou D, Mu Y, Zhang Y, Zhao C, Liu S, Chi Z, Xu J, Wu YC, Lu PY, Lien A, Bryce MR. *Angew Chem Int Ed*, 2016, 55: 2181–2185
17 Yang J, Zhen X, Wang B, Gao X, Ren Z, Wang J, Xie Y, Li J, Peng Q, Pu K, Li Z. *Nat Commun*, 2018, 9: 840
18 Li Q, Li Z. *Acc Chem Res*, 2020, 53: 962–973
19 Salla CAM, Farias G, Rouzières M, Dechambenoit P, Durola F, Bock H, de Souza B, Bechtold IH. *Angew Chem Int Ed*, 2019, 58: 6982–6986
20 Yang J, Fang M, Li Z. *Aggregate*, 2020, 1: 6–18
21 Li D, Lu F, Wang J, Hu W, Cao XM, Ma X, Tian H. *J Am Chem Soc*, 2018, 140: 1916–1923
22 Wang J, Huang Z, Ma X, Tian H. *Angew Chem Int Ed*, 2020, 59: 9928–9933
23 Lei Y, Dai W, Guan J, Guo S, Ren F, Zhou Y, Shi J, Tong B, Cai Z, Zheng J, Dong Y. *Angew Chem Int Ed*, 2020, 59: 16054–16060
24 Shi H, An Z. *Nat Photon*, 2019, 13: 74–75
25 Kabe R, Adachi C. *Nature*, 2017, 550: 384–387
26 Zhang X, Du L, Zhao W, Zhao Z, Xiong Y, He X, Gao PF, Alam P, Wang C, Li Z, Leng J, Liu J, Zhou C, Lam JWY, Phillips DL, Zhang G, Tang BZ. *Nat Commun*, 2019, 10: 5161
27 Aonuma M, Oyamada T, Sasabe H, Miki T, Adachi C. *Appl Phys Lett*, 2007, 90: 183503
28 Wang Y, Yang J, Fang M, Yu Y, Zou B, Wang L, Tian Y, Cheng J, Tang BZ, Li Z. *Matter*, 2020, 3: 449–463
29 Kuila S, George SJ. *Angew Chem Int Ed*, 2020, 59: 9393–9397
30 Tian Y, Yang X, Gong Y, Wang Y, Fang M, Yang J, Tang Z, Li Z. *Sci China Chem*, 2020, 64: 445–451
31 Deng R, Wang J, Chen R, Huang W, Liu X. *J Am Chem Soc*, 2016, 138: 15972–15979
32 Sun Y, Giebink NC, Kanno H, Ma B, Thompson ME, Forrest SR. *Nature*, 2006, 440: 908–912
33 Sugiyama K, Yoshimura D, Miyamae T, Miyazaki T, Ishii H, Ouchi Y, Seki K. *J Appl Phys*, 1998, 83: 4928–4938
34 Fries F, Louis M, Scholz R, Gmelch M, Thomas H, Haft A, Reineke S. *J Phys Chem A*, 2020, 124: 479–485
35 Hirata S. *J Mater Chem C*, 2018, 6: 11785–11794
36 Wang H, Yue B, Xie Z, Gao B, Xu Y, Liu L, Sun H, Ma Y. *Phys Chem Chem Phys*, 2013, 15: 3527–3534
37 Főrster T. *Discuss Faraday Soc*, 1959, 27: 7–17
38 Förster T. *Ann Phys*, 1948, 437: 55–75
39 Yu X, Zhang H, Yu J. *Aggregate*, 2021, 2: 20–34